International Journal of Offshore and Polar Engineering (ISSN 1053-5381)

Vol. 35, No. 2, June 2025, pp. 168–176; https://doi.org/10.17736/ijope.2025.ak73

http://www.isope.org/publications

Two-Way Coupled CFD-FEA Method for Dam-Break Flows Impacting on the Elastic Beam

Jiawei Xiao*
Computational Marine Hydrodynamics Lab (CMHL), School of Naval Architecture Ocean and Civil Engineering, Shanghai Jiao Tong University, Shanghai, China

Xiao Wen
Marine Design and Research Institute of China
Shanghai, China

Jianhua Wang* and Decheng Wan*†
Computational Marine Hydrodynamics Lab (CMHL), School of Naval Architecture Ocean and Civil Engineering, Shanghai Jiao Tong University, Shanghai, China

Ships sailing in rough seas will encounter phenomena, such as green water, which could be simplified as a dam break problem. The phenomena will cause structural deformation by impacting loads from wave and sea dilaters. This paper proposes a two-way coupled Computational Fluid Dynamics-Finite Element Analysis (CFD-FEA) method to study the impact of a dam break flow on a stiffened elastic beam. The method is constructed based on preCICE, which is an open-source coupling library for partitioned multi-physics simulations. The flow field is solved by the Reynolds-averaged Navier-Stokes method with OpenFOAM, and the structural part is solved by FEA with Calculix. The effect of longitudinal bone reinforcement is studied in this paper. The results indicate that the method can effectively simulate the influence of longitudinal bone, which can reduce the deformation of beams, consistent with the design of wave deflectors.

INTRODUCTION

In rough sea conditions, the green water phenomenon could cause large slamming loads over a short duration. This phenomenon can often be numerically simulated by a dam break problem, which is more prevalent than a plunging wave in ocean engineering (Greco et al., 2007). The slamming loads in a dam break problem will cause severe structural damage. Hence, investigating slamming loads and the hydroelastic response is very important for practical engineering designs.

Researchers have conducted experiments and numerical simulations to study the interactions between elastic beams and water. Traditionally, the Finite Volume Method (FVM), Finite Element Method (FEM), and Finite Difference Method (FDM) are commonly used to address Fluid-Structure Interaction (FSI) problems. Walhorn et al. (2005) conducted a series of two-dimensional dam break experiments. They proposed a numerical method to analyze the FSI between the water and the elastic beam using the mesh method. Modified ansatz functions were introduced to consider discontinuities. Liao et al. (2015) found that large slamming loads, whipping, and rough flow are the main phenomena in their quasi-two-dimensional experiment. They also used the FDM-FEM method to simulate the results. However, the mesh dependence and the convergence problem were unstable. Yilmaz et al. (2021) used the digital video images to calculate the displacements of the elastic gate and free surface evolution at their newly designed experiment. Attili et al. (2023) used the FVM to simulate wave impact on flexible baffles, analyzed the interaction phenomena between fluids and solids, and verified the effectiveness of the program through physical experiments.

Other researchers have proposed numerical methods and compared their results with the experiment benchmark for validation. A CFD-CSM method was proposed by Hu et al. (2023) to study the elastic response of vertical walls in ocean waves. Elastic material decreases the wave reflection and loads compared with rigid material.

However, the large deformation may cause divergence using the mesh method. To overcome the problem, some scholars considered the immersed boundary method (IBM) to handle such coupling. Several works adopt the IBM to solve FSI problems and model the interface boundary. Jiang et al. (2021), Yang et al. (2022), Xin et al. (2023), and Zhao et al. (2024) proposed the IBM-FDEM method to study the problem. A dam break through an elastic gate was introduced to validate the problem and prove that the method is accurate. Other CFD-CSM methods have been used in the water-entry problem to study ship hydroelasticity (Jiao et al., 2024; Xiao et al., 2024; Zhang et al., 2025).

Lagrangian meshfree methods (particle methods) have been used in the following studies. Ryzhakov et al. (2010) proposed a numerical FSI method based on a Lagrangian description. The fluid part calculation is a linear interpolation, while the structure formulation is based on displacement. A series of numerical examples were applied to validate the proposed method, including dam failure examples. Khayyer et al. (2018, 2024) and Shimizu et al. (2022) developed Smoothed Particle Hydrodynamics (SPH)-based FSI solvers based on purely meshfree Lagrangian frameworks for both fluid and structure. The dam break through an elastic gate verified the validation of the method.

Zheng et al. (2020) proposed an MPS model to simulate the FSI problem. The structural element was used as ghost cells in

*ISOPE Member; † Corresponding author.

Received October 28, 2024; updated and further revised manuscript received by the editors December 27, 2024. The original version (prior to the final updated and revised manuscript) was presented at the Thirty-fourth International Ocean and Polar Engineering Conference (ISOPE-2024), Rhodes, Greece, June 16–21, 2024.

KEY WORDS: Two-way coupled, CFD-FEA method, dam break, elastic beam.

the GCB model. Dam break and water in the rotating test were conducted to validate the efficiency and accuracy of the method. Zhang et al. (2022) proposed two interpolation methods within the MPS-FEM method, including the SFBI and KFBI, to solve the partitioned FSI simulation which is validated by two-dimension FSI cases. Wu et al. (2022) introduced the mixed-mode function to the MPS method, and the elastic wave dam break case is used to validate the problem. McLoone et al. (2022) proposed a new FVPM-FE method which can independently chose the particle size without considering the structure thickness. They made sure that particles interacted with the right neighbor instead of overlapping the thin structure.

In addition to IBM and particle methods, there is still room for improvement to the ordinary grid FVM method. The current direction of consideration is mainly to reduce mesh deformation, such as introducing overlapping mesh methods. This article uses mainly the dynamic grid method to verify the proposed CFD-FEM method, which serves as a validation for the subsequent introduction of overlapping grid methods. The numerical results are compared with the experiment results to verify its application. The effects of the bones are discussed.

NUMERICAL METHOD

In this section, a two-way coupled CFD-FEA method is proposed to investigate the dam break problem. The main framework of the coupling is discussed in this section. The fluid domain is solved by OpenFOAM (Jasak, 1996; Rusche, 2002) with the Reynolds-averaged Navier-Stokes (RANS) model and Volume of Fluid (VOF) method. Calculix, an open-source FEA software, is employed to solve the structure part. The coupling library for partitioned multi-physics simulations, known as preCICE, is utilized to couple the fluid part with the structure part in a strongly implicit way.

Fluid Part

The interFoam solver in OpenFOAM ESI v2306 is employed in the fluid part. The dynamic mesh method is adopted in the solver. OpenFOAM uses the PIMPLE algorithm—a combination of the Pressure-Implicit with Splitting of Operators (PISO) algorithm and the Semi-Implicit Method for Pressure Linked Equations (SIMPLE) algorithm—to decouple velocity and pressure.

The use of incompressible models to study the dam break problem is a common as well as stable approach in the current research field. The equations of the RANS method are shown as follows:

$$\nabla \cdot \boldsymbol{U} = 0 \tag{1}$$

$$\frac{\partial \rho \boldsymbol{U}}{\partial t} + \nabla \cdot [\rho(\boldsymbol{U} - \boldsymbol{U}_g)\boldsymbol{U}] = -\nabla p_d - \boldsymbol{g} \cdot \boldsymbol{x} \nabla \rho + \nabla \cdot (\mu_{\text{eff}} \nabla \boldsymbol{U}) + (\nabla \boldsymbol{U}) \cdot \nabla \mu_{\text{eff}} + \boldsymbol{f}_\sigma + \boldsymbol{f}_s \tag{2}$$

In the equation above, $\boldsymbol{U}$ is the velocity field; $\boldsymbol{U}_g$ is the grid moving speed; $p_d = p - \rho g \cdot x$ is the fluid dynamic pressure; $\boldsymbol{x}$ is the fluid coordinate position vector; ρ is the density of liquid or gas; $\boldsymbol{g}$ is the gravitational acceleration vector; and $\mu_{\text{eff}} = \rho(v + v_t)$ is the effective dynamic viscosity, where v and v_t are called kinematic viscosity and turbulent eddy viscosity, respectively, and the latter is solved by the turbulence model; $\boldsymbol{f}_\sigma$ is the surface tension term in the two-phase flow model, and $\boldsymbol{f}_s$ is the source term applied in the extinction region. k-ω SST model (Menter et al., 2009) is used to solve the turbulent eddy viscosity v_t.

When it comes to the free surface capture, the VOF method (Berberović et al., 2009) with artificial compression is used to solve the problem. The transport equation of the phase fraction is

$$\frac{\partial \alpha}{\partial t} + \nabla \cdot [(\boldsymbol{U} - \boldsymbol{U}_g)\alpha] + \nabla \cdot [\boldsymbol{U}_r(1-\alpha)\alpha] = 0 \tag{3}$$

where α is the phase fraction between 0 and 1. Different values of α represent the following meanings:

$$\begin{cases} \alpha = 0 & \text{air} \\ \alpha = 1 & \text{water} \\ 0 < \alpha < 1 & \text{interface} \end{cases} \tag{4}$$

Structural Part

The structural responses of the beam are calculated using Calculix, a free three-dimensional structural finite element program that makes use of the Abaqus input format. It is possible to use commercial pre-processors. The four-node continuum shell element (S4R) and eight-node brick element with reduced integration solid element (C3D8R) is used to discretize the wedge structure. One end of the beam is fixed to form a cantilever beam structure. The dynamic movement of the wedge is described via displacement field u and the equation is shown below.

$$M\ddot{\boldsymbol{u}} + C\dot{\boldsymbol{u}} + K\boldsymbol{u} = \boldsymbol{q} \tag{5}$$

where M, K, and C are the structure mass, stiffness, and damping $n \times n$ matrix. The damping matrix used Rayleigh damping, which is a linear combination of mass and stiffness of the structure. The dynamic equation is solved by generalized alpha method.

Two-way Coupled Method

In this paper, the multi-physics field coupling library preCICE (Chourdakis et al., 2022) is used to couple the above fluid solver with the structure solver to achieve a two-way coupled solver. preCICE is an open-source massively parallel system-based coupling library for partitioned multi-physics field simulations jointly developed by the Technical University of Munich and the University of Stuttgart in Germany using C++. It is powerful enough to be used as a third-party coupling tool to couple OpenFOAM flow field calculations with other open-source FEM solvers, such as Calculix (Uekermann et al., 2017; Chourdakis et al., 2023). This approach has been successfully applied to study the fluid-structure interaction problems in water-entry slamming (Xiao et al., 2024) and ship hydroelasticity (Zhang et al., 2025). For coupling solutions, preCICE uses an adapter as an interface to interpolate and exchange data directly without modifying the underlying code, just by calling the libpreCICE library in each open-source program. The coupled diagram based on preCICE is shown in Fig. 1.

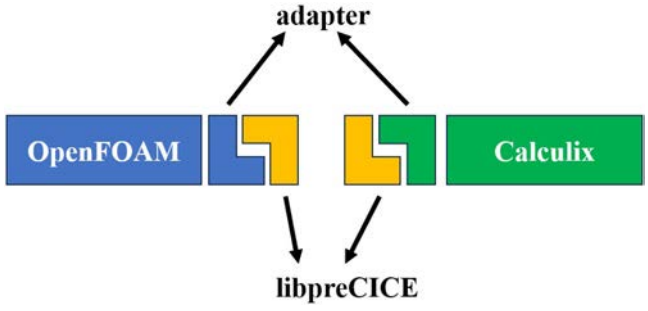

Fig. 1 Schematic diagram of preCICE data exchange

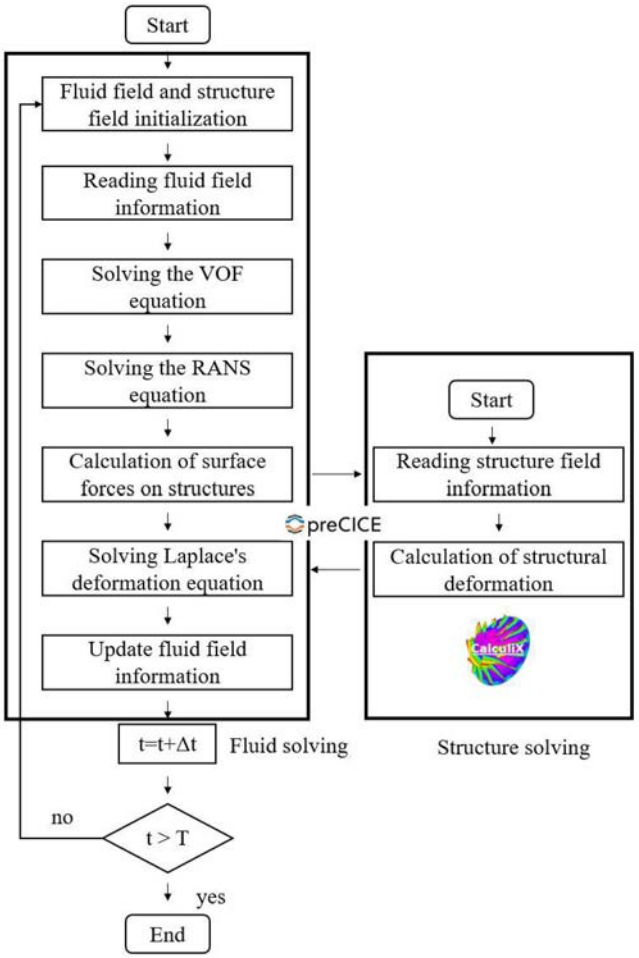

Fig. 2 FSI solver flowchart

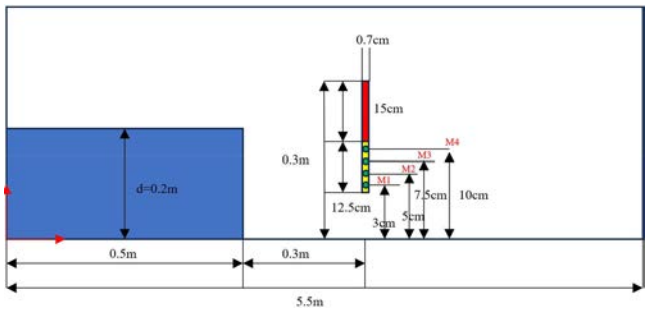

Fig. 3 Schematic of the numerical flume

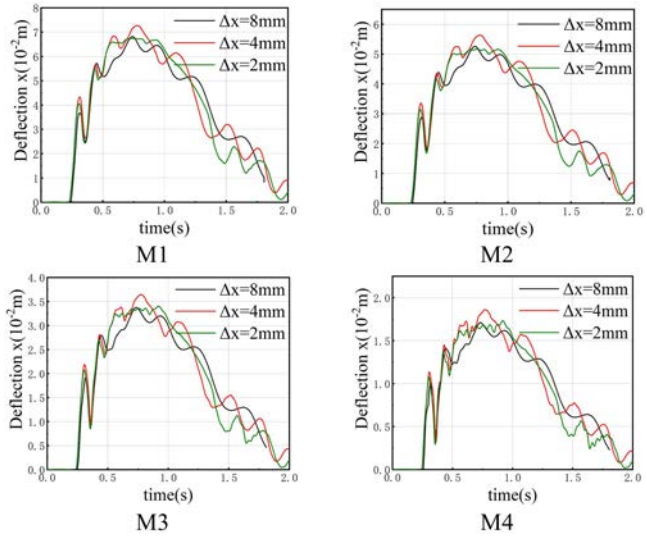

Fig. 4 Effect of mesh sensitivity

As shown in Fig. 2, the FSI solver calculates the forces on the surface of the structure in the fluid solver section and passes them onto the structure solver module via preCICE. Calculix calculates the structural deformation caused by the structural forces and then passes it back to the fluid solver module to solve the Laplace deformation equation to update the shape of the body mesh, realizing a two-way coupling. preCICE uses the RBF method to map the force and displacement between OpenFOAM and Calculix. RBF, which is short for radial basis function mapping, computes the global interaction between fluid and solid mesh. There are several models to choose for the RBF method to map the problem. This paper uses rbf-compact-tps-c2 to do the mapping work. We also need acceleration techniques to stabilize and accelerate the fixed-point iteration. PreCICE offers three different acceleration methods. We choose IQN-ILS (aka Anderson acceleration) to accelerate the work. The maximum iterations are 20 within a single time step.

NUMERICAL SIMULATIONS

Validation of CFD-FEA Method

The experiment conducted by Yilmaz et al. (2021) is used as the first test case for validating the CFD-FEA method. The simulation results would be compared with the δ-TL-SPH model work of Chen et al. (2024). The numerical water tank is 5.5 m long, as shown in Fig. 3. The water column is 0.2 m deep and 0.5 m long. The elastic plate, which is 0.275 m long and 0.007 m thick, is installed at 0.3 m right next to the water column. Rigid and elastic plates are colored in red and yellow, respectively. The material is density 1,250 kg/m^3; Poisson's ration is 0.4, and Young's modulus is 4 MPa. Four measurement points are placed on the plate.

Three different fluid meshes are considered to investigate their sensitivity. The size of the mesh includes 2 mm, 4 mm, and 8 mm (coarse, medium, and fine, respectively). Figure 4 shows the effect of mesh sensitivity at the four points measured. The three mesh deflection time courses are relatively similar. The medium is a larger peak at the first peak. The fine mesh is smoother during the development phase from 0.5 s to 1.0 s. This is because the flow field is unstable due to the sparse mesh and therefore, the structural response oscillates more. To ensure that the flow field calculation is stable, we use fine mesh as the fluid field grid in this paper.

A comparison of the calculated results with the two particle spacings, from the literature and the experimental results, is shown in Fig. 5.

The relative error shown in Table 1 between the CFD-FEA method and the experimental results is less than 3.8% and lower than the literature's result at M1–M3. The second peak's result of numerical results is in good agreement with the literature and with the experiment, while the first peak is smaller, which may be caused by the movement of the tank gate. Therefore, the lack of simulation for gates may cause this discrepancy. The results of the CFD simulations produce large oscillations during the development phase after 1.0 s. This may be related to the situation where the dam-busting flow rolls over after contacting the elastic plate and becomes entangled in the air. Figure 6 shows the fluid domain of the CFD-FEA results compared with Chen et al.'s (2024) results. Compared to single-phase flow methods, CFD methods for multiphase flow capture phenomena such as

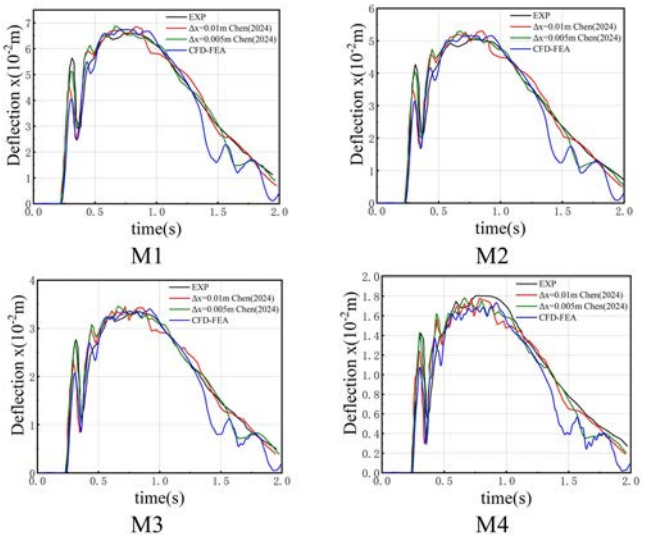

Fig. 5 Comparison of the deflection

Simulation method	Max top displacement	Relative error
M1		
CFD-FEA	6.7379 cm	2.0%
$\Delta x = 0.01$ m SPH	6.8650 cm	3.9%
$\Delta x = 0.005$ m SPH	6.8520 cm	3.7%
EXP	6.6060 cm	/
M2		
CFD-FEA	5.1569 cm	1.3%
$\Delta x = 0.01$ m SPH	5.3040 cm	4.2%
$\Delta x = 0.005$ m SPH	5.2770 cm	3.7%
EXP	5.0900 cm	/
M3		
CFD-FEA	3.4016 cm	1.5%
$\Delta x = 0.01$ m SPH	3.4506 cm	3.0%
$\Delta x = 0.005$ m SPH	3.4587 cm	3.2%
EXP	3.3506 cm	/
M4		
CFD-FEA	1.7324 cm	–3.8%
$\Delta x = 0.01$ m SPH	1.7784 cm	–1.2%
$\Delta x = 0.005$ m SPH	1.7828 cm	–1.0%
EXP	1.8001 cm	/

Table 1 Structural deformation results of different methods at M1–M4

entrapped air bubbles. The bubble caused by the consideration of multiphase free surface may have an important influence in the progress of the dam break impact and deformation.

Another validation case conducted by Idelsohn et al. (2008) and Yang et al. (2016) is introduced in this section to investigate the interaction between a dam break and an elastic structure. The two-dimensional fluid domain is 0.584 m long and 0.4 m high. The water volume is 0.292 m long and 0.146 m wide. The beam's structure is 0.0012 m × 0.08 m. It is located 0.146 m downstream from the end of the water volume. As shown in Fig. 7, all boundaries are treated as walls with no-slip conditions, except for the top boundary, which is considered an atmosphere boundary with free inlet and outlet flow.

The structural parameters are shown in Table 2. Young's modulus E of the structure is 1 MPa, with density $\rho = 2.5 \times 10^3$ kg/m^3. The passion ratio is 0. A relatively small Young's modulus of

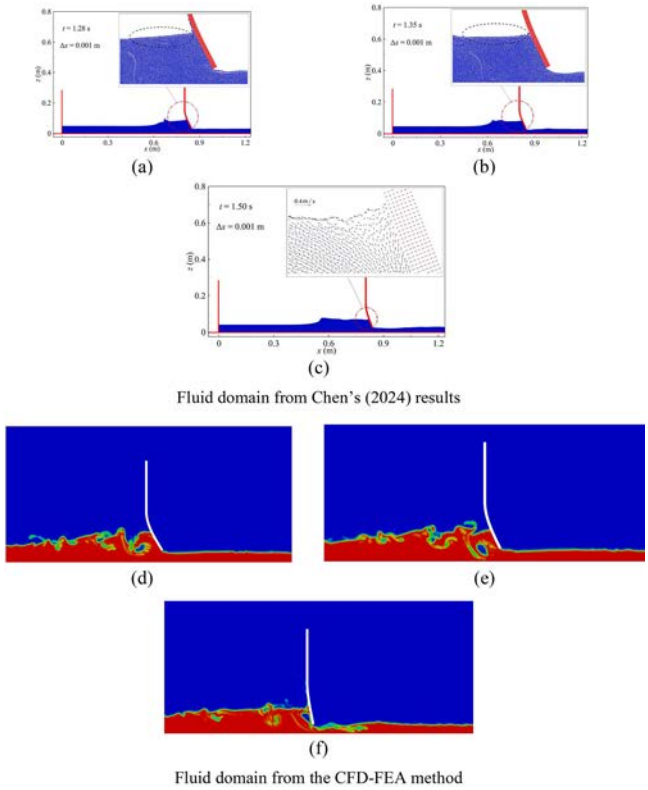

Fig. 6 Comparison of the fluid domain

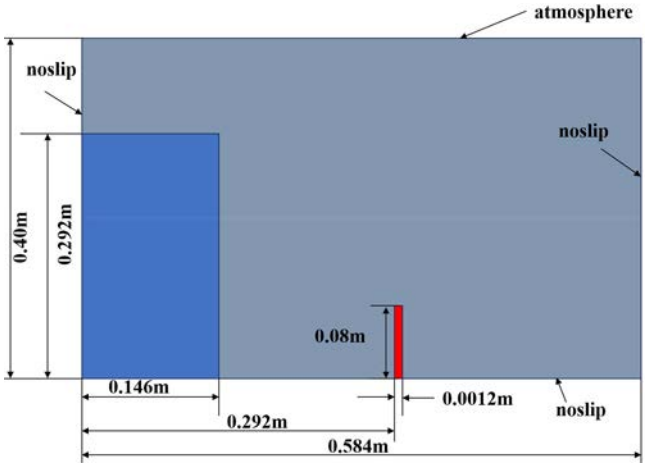

Fig. 7 Diagram of the numerical setup for the dam break test case

the structure means that the structural beam is relatively soft and therefore undergoes significant deformation during the impact of dam break flow. Due to the use of dynamic mesh updating in this method, the large deformation at the top of the secondary beam may lead to a decrease in mesh quality, which in turn may cause computational divergence. To ensure the convergence of calculations and smooth coupling, the calculation time step is set to 0.0002 s.

Parameter	Value
E	1 MPa
ρ	2.5×10^3 kg/m^3
Poisson's ratio	0
Δt	0.0002 s

Table 2 Parameter settings of fluid and structure simulations

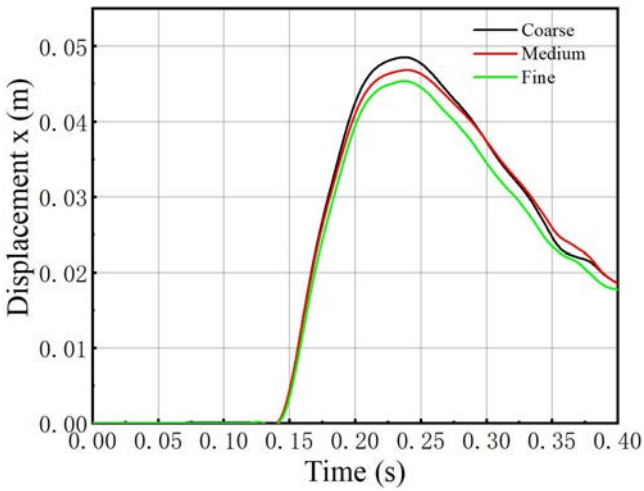

Fig. 8 Comparison of the horizontal top displacement of beam with three different meshes

Cell type	Max top displacement	Relative error
Coarse	0.04851 m	6.9%
Medium	0.04681 m	2.3%
Fine	0.04536 m	/

Table 3 Structural deformation results of different cell type

To investigate the sensitivity of the fluid mesh, three cell sizes, 2 mm, 4 mm, and 6 mm, are adopted in this simulation. The numerical time results of the top horizontal displacements in the structure are further compared with three meshes, as shown in Fig. 8. It could be concluded that all three meshes maintain a favorable time history for the top beam displacement and exhibit relatively small computational errors in peak value. Table 3 presents the specific numerical values of each mesh and the error relative to the fine mesh. The coarse mesh presents the maximum displacement at the top, as the beam becomes softer. This phenomenon may be caused by a larger interpolation error between the coarse mesh force and displacement. For the sake of computational efficiency, the medium sized grid with 11,160 cells is adopted.

To further discuss the time step interval, we choose three different time steps (0.001 s, 0.0005 s, and 0.0002 s). As shown in Fig. 9 and Table 4, the relative error of the different time steps remains less than 2.3%, which means the time steps converge. To accelerate the progress, we choose 0.001 s as the time step for simulation.

The horizontal displacements of the free end of the flexible beam are shown in Fig. 10, compared with the results obtained by the particle finite element method (PFEM; Idelsohn et al., 2008) and the Smoothed Particle Hydrodynamics-Element Bending Group method (Yang et al., 2016). The time history of the horizontal displacements of the CFD-FEA method is in good agreement with the results of the literature. As Table 5 shows, the maximum top displacement of the CFD-FEA is 0.04681 m. Compared with Idelsohn and Yang's results, the relative error is lower than 1.35%.

Figure 11 compares the CFD-FEA method with the flow field evolution in the above literature. At 0.16 s, the water climbed along the beam. The middle of the beam first experienced a large horizontal displacement, while the free end of the beam maintained its original position due to inertia, resulting in a bow shape. At the same time, the jet splashed out along the beam, causing fragmentation. At 0.34 seconds, the jet splashed onto the right

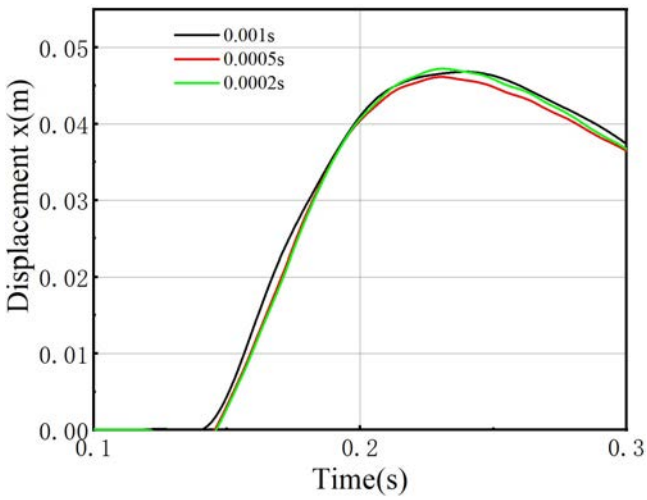

Fig. 9 Comparison of the horizontal top displacement of beam with three different time steps

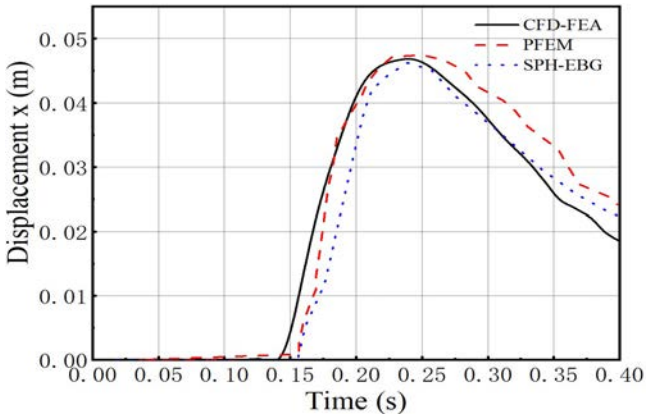

Fig. 10 Comparison of the top displacement of beam with different methods

Time step	Max top displacement	Relative error
0.001 s	0.04681 m	0.9%
0.0005 s	0.04614 m	2.3%
0.0002 s	0.04724 m	/

Table 4 Structural deformation results of different time step

Simulation method	Max top displacement	Relative error
CFD-FEA	0.04681 m	/
PFEM	0.04745 m	1.35%
SPH-EBG	0.04622 m	1.28%

Table 5 Structural deformation results of different methods

wall, generating the peak slamming pressure. At this point, all the water was loaded on the left side of the beam, causing the beam to bend. However, due to the maximum impact pressure already leaving the surface of the beam, the deformation of the beam was slightly reduced.

Overall, the structural response and flow field results obtained from CFD-FEA numerical simulation are highly consistent with results of the literature. This verifies that the proposed CFD-FEA method is applicable to the study of elastic beam dam failure.

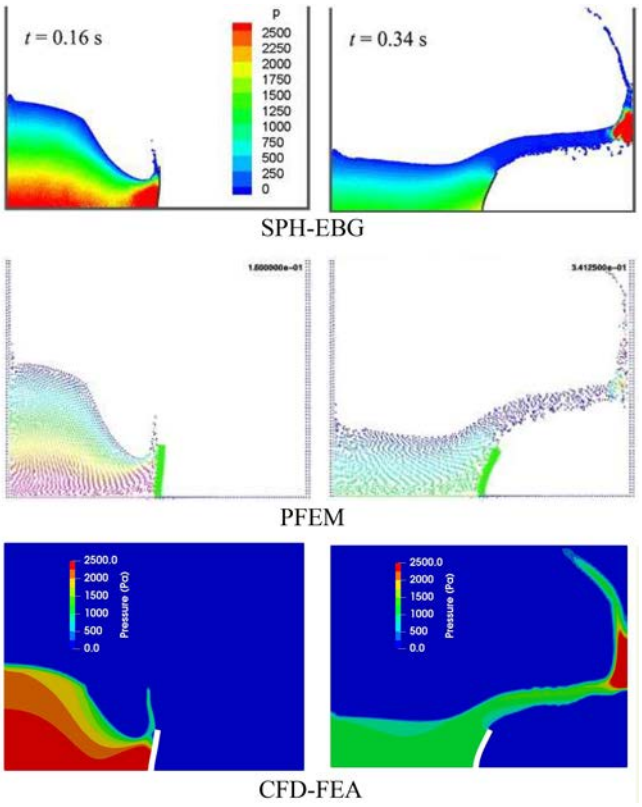

Fig. 11 Comparison of CFD-FEA simulation with PFEM and SPH–EBG results at time 0.16 s, 0.34 s. The color shows the pressure of the fluid.

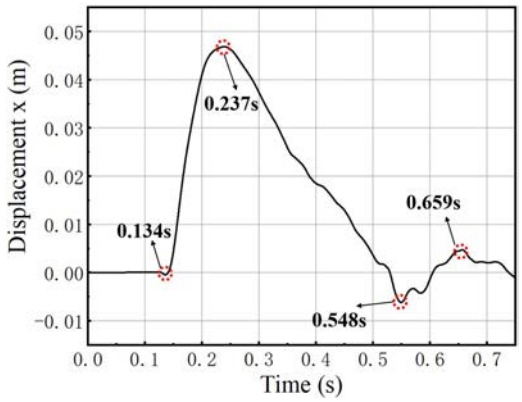

Fig. 12 Time history of horizontal displacement

Evolution of the Fluid Domain

This section focuses on the relationship between the time history of displacement at the top of an elastic beam at the time of impact in a dam break flow and the spatiotemporal distribution of the impact load. Some pressure slices at specific displacement moments are compared and analyzed. Figure 12 shows the time history of horizontal displacement. Four moments are selected from the figure. At 0.134 s, the beam bends 0.00043 m in the negative x-axis direction before starting to deform. At 0.237 s, the beam reaches its maximum deformation value of 0.04681 m. At 0.548 s, after deformation and recovery, the beam shifts 0.00612 m towards the negative x-axis direction. At 0.657 s, the beam is offset in the positive direction of the x-axis by 0.00475 m.

Figure 13 shows the pressure distribution in the flow field at different times. At 0.134 s, the dam break flow has not yet climbed to half of the elastic beam, and the deformation of the elastic beam is caused by the large impact pressure. The deformation develops from the fixed end to the free end, and the position of the maximum deformation coincides with the development of the root of spray. At 0.237 s, the horizontal displacement at the free end reaches its maximum value. At this point, the jet crosses the elastic beam and develops towards the right wall. The extreme pressure is concentrated at the root, and the dominant factor promoting horizontal deformation becomes the gravity of water loaded on the surface of the elastic beam. At 0.548 s, the water on the elastic beam decreases and at the same time, the water on the right wall is slammed and flows back, causing the beam to rebound on the right side. At 0.659 seconds, after the backflow of water slams, the large amount of residual water loaded on the left side regains control, causing the elastic beam to oscillate with great amplitude back and forth until the water finally stabilizes. When the dam break floods over the elastic plate, it creates the phenomenon of generating bubbles that mix in with the air.

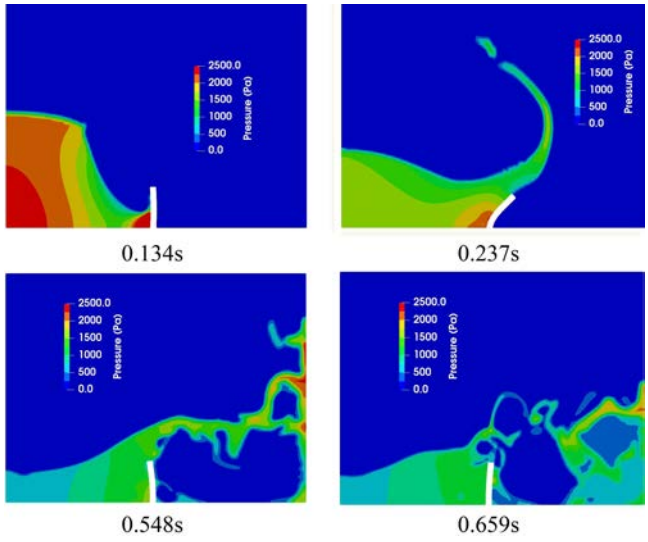

Fig. 13 Pressure snapshot at different moments

Effects of Longitudinal Bone Reinforcement

To reduce the impact of wave slamming, ships will install wave deflectors on their decks. Longitudinal bones are usually added to strengthen the wave board. This section investigates the effect of longitudinal bone reinforcement on the deformation of elastic beams after a dam break. The structural modeling is shown in Fig. 14. The main unit of the beam is modeled using solid elements of C3D8R, while the longitudinal beam is modeled using

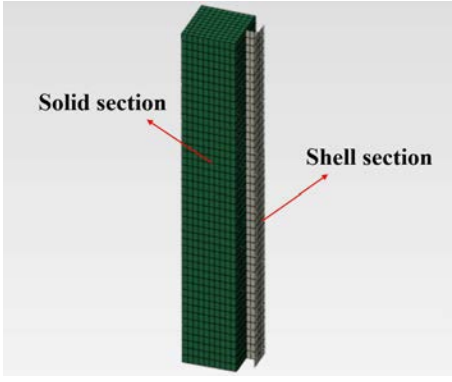

Fig. 14 Structural modeling of the stiffened beam

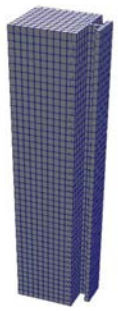

Fig. 15 Structural cells involved in calculations

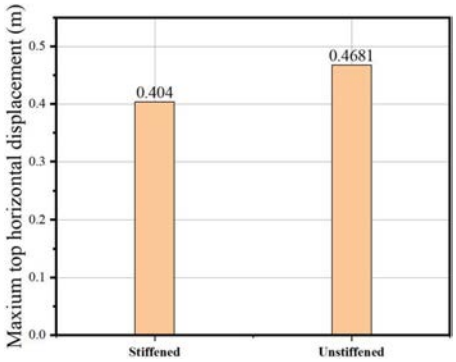

Fig. 16 Maximum top horizontal displacement of stiffened and unstiffened beams

shell elements of S4R. The material setting of the longitudinal bone is the same as the main body of the beam, with a thickness of 0.0005 m. Calculix elevates the shell elements to solid elements based on thickness settings during the calculation process, as shown in Fig. 15. The time step remains 0.0002 s.

Figure 16 shows the comparison of the maximum top horizontal displacement between the stiffened and unstiffened beams. The presence of longitudinal bones reduces the horizontal displacement at the top. The relative error is approximately 13.7%. From the flow field diagram in Fig. 17, the displacement cloud map of the beam shows that the large displacement area of the reinforced

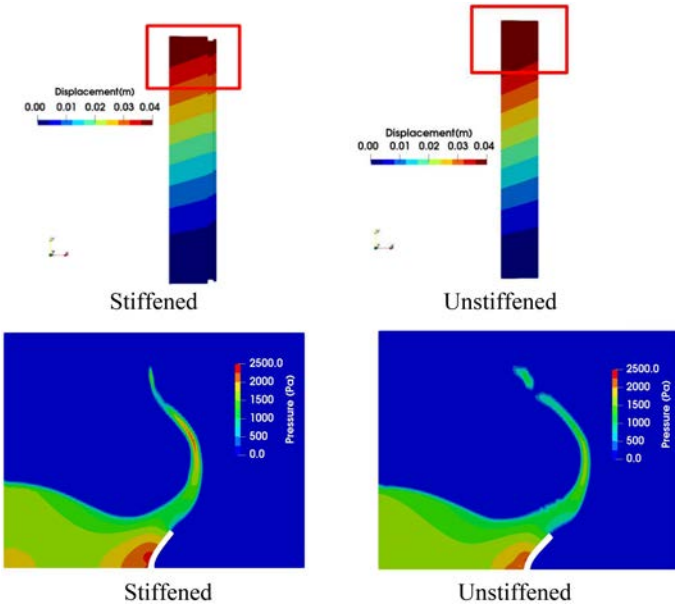

Fig. 17 Top horizontal displacement of stiffened and unstiffened beams

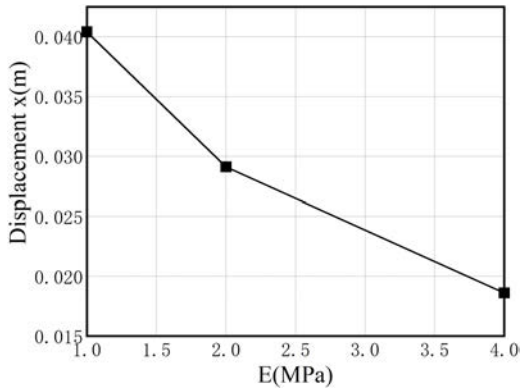

Fig. 18 Horizontal top displacement of beam with three different materials

E	Max top displacement	Decrease
1 MPa	0.0404 m	/
2 MPa	0.0291 m	0.0113 m
3 MPa	0.0186 m	0.0105 m

Table 6 Structural deformation for different materials

plate beam decreases. The peak pressure is still concentrated at the root when it reaches its peak. Currently, the dominant factor causing the deformation of the beam is still the gravitational load of water, which is consistent with the situation without the addition of a beam.

It can be seen in Fig. 18 and Table 6 that longitudinal bone strengthening has a nonlinear effect. The larger the material E, the smaller the change in horizontal deformation, which may eventually approach zero. This means that simply strengthening the longitudinal bone has its limitations, so in-depth research should be conducted from the shape of the longitudinal bone and the plate itself. Figure 19 shows the stress distribution of the stiffened beam with different materials. The large deformation of the beam causes the longitudinal bones to become wavy from the fixed end. The maximum stress is concentrated at the fixed end and the bottom of the web plate. The maximum longitudinal stress at the fixed end of the three materials is $E = 4$ MPa.

CONCLUSIONS

This paper has proposed a two-way coupled CFD-FEA method, which combines the interFoam solver in OpenFoam v2306 with the finite element solver, Calculix. The open-source multi-physics coupling library preCICE is introduced in this paper to do the communication and coupled work. Validation is carried out for two benchmark examples of an elastic beam in a dam break problem. The relative error between the CFD-FEA method and the Chen et al. (2024) results is less than 3.8%. The error between the top displacement obtained from numerical simulation and the literature (Idelsohn et al., 2008; Yang et al., 2016) is less than 1.35%. The flow field evolution is also in good agreement with the results in the literature. The results show the applicability of the solver for simulating structural responses of the elastic beam in a dam break problem.

The evolution of a dam break flow field considering elastic beams was also investigated. Compared to single-phase flow methods, CFD methods for multiphase flow can capture phenomena, such as entrapped air bubbles. A bubble caused by the consideration of the multiphase free surface has an important influence in the progress of the dam break impact and deformation.

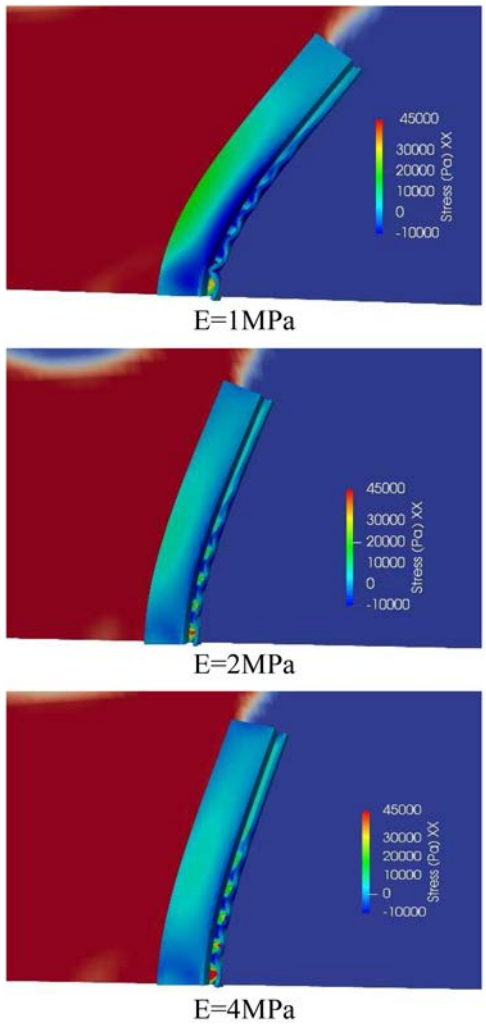

Fig. 19 Beam stress from three different materials

Flow field analysis has shown that as the dam break flow develops, the elastic beam will oscillate under the impact of water flow on both sides. A solution has been developed to investigate the effect of longitudinal bone reinforcement on the deformation of elastic beams in a dam break problem. The results show that the longitudinal reinforcement method can effectively reduce the top displacement of elastic beams under the impact of a dam break flow. The analysis results further validate the current design concept for a ship's wave blocking beams.

Future work will focus on the material of beams and the influence of longitudinal or transverse bone arrangement methods.

ACKNOWLEDGEMENTS

This work is supported by the National Natural Science Foundation of China (52471335, 52131102), to which the authors are most grateful.

REFERENCES

Attili, T, Heller, V, and Triantafyllou, S (2023). "Wave Impact on Rigid and Flexible Plates," *Coastal Eng*, 182, 104302. https://doi.org/10.1016/j.coastaleng.2023.104302.

Berberović, E, van Hinsberg, N, Jakirlić, S, Roisman, I, and Tropea, C (2009). "Drop Impact onto a Liquid Layer of Finite Thickness: Dynamics of the Cavity Evolution," *Phys Rev E*, 79(3), 36306. https://doi.org/10.1103/PhysRevE.79.036306.

Chen, YK, Meringolo, DD, and Liu, Y (2024). "SPH Numerical Model of Wave Interaction with Elastic Thin Structures and its Application to Elastic Horizontal Plate Breakwater," *Mar Struct*, 93, 103531. https://doi.org/10.1016/j.marstruc.2023.103531.

Chourdakis, G, Davis, K, Rodenberg, B, et al. (2022). "Precice V2: A Sustainable and User-Friendly Coupling Library," *Open Res Eur*, 2, 51. https://doi.org/10.12688/openreseurope.14445.2.

Chourdakis, G, Schneider, D, and Uekermann, B (2023). "OpenFOAM-preCICE: Coupling OpenFOAM with External Solvers for Multi-Physics Simulations," *OpenFOAM® J*, 3, 1–25. https://doi.org/10.51560/ofj.v3.88.

Greco, M, Colicchio, G, and Faltinsen, OM (2007). "Shipping of Water on a Two-Dimensional Structure. Part 2," *J Fluid Mech*, 581, 71–99. https://doi.org/10.1017/S002211200700568X.

Hu, Z, Huang, L, and Li, Y (2023). "Fully-coupled Hydroelastic Modeling of a Deformable Wall in Waves," *Coastal Eng*, 179, 104245. https://doi.org/10.1016/j.coastaleng.2022.104245.

Idelsohn, SR, Marti, J, and Limache, A (2008). "Unified Lagrangian Formulation for Elastic Solids and Incompressible Fluids: Application to Fluid–Structure Interaction Problems Via the PFEM," *Comput Methods Appl Mech Eng*, 197(19), 1762–1776. https://doi.org/10.1016/j.cma.2007.06.004.

Jasak, H (1996). *Error Analysis and Estimation for the Finite Volume Method with Applications to Fluid Flows*, PhD Thesis, Imperial College, London, UK.

Jiang, F, Matsumura, K, Ohgi, J, and Chen, X (2021). "A GPU-Accelerated Fluid–Structure-Interaction Solver Developed by Coupling Finite Element and Lattice Boltzmann Methods," *Comput Phys Comm*, 259, 107661. https://doi.org/10.1016/j.cpc.2020.107661.

Khayyer, A, Gotoh, H, Falahaty, H, and Shimizu, Y (2018). "An Enhanced ISPH–SPH Coupled Method for Simulation of Incompressible Fluid–Elastic Structure Interactions," *Comput Phys Commun*, 232, 139–164. https://doi.org/10.1016/j.cpc.2018.05.012.

Khayyer, A, Gotoh, H, Shimizu, Y, and Gotoh, T (2024). "An Improved Riemann SPH-Hamiltonian SPH Coupled Solver for Hydroelastic Fluid-Structure Interactions," *Eng Anal Bound Elem*, 158, 332–355. https://doi.org/10.1016/j.enganabound.2023.10.018.

Liao, K, Hu, C, and Sueyoshi, M (2015). "Free Surface Flow Impacting on an Elastic Structure: Experiment Versus Numerical Simulation," *Appl Ocean Res*, 50, 192–208. https://doi.org/10.1016/j.apor.2015.02.002.

Mcloone, M, and Quinlan, NJ (2022). "Coupling of the Meshless Finite Volume Particle Method and the Finite Element Method for Fluid–Structure Interaction with Thin Elastic Structures," *Eur J Mech B/Fluids,* 92, 117–131. https://doi.org/10.1016/j.euromechflu.2021.12.001.

Menter, FR (2009). "Review of the Shear-Stress Transport Turbulence Model Experience from an Industrial Perspective," *Int J Comput Fluid Dyn*, 23(4), 305–316. https://doi.org/10.1080/10618560902773387.

Rusche, H (2002). *Computational Fluid Dynamics of Dispersed Two-phase Flows at High Phase Fractions*, PhD Thesis, Imperial College, London, UK.

Ryzhakov, PB, Rossi, R, Idelsohn, SR, and Onate, E (2010). "A Monolithic Lagrangian Approach for Fluid–Structure Interaction Problems," *Comput Mech*, 46, 883–899. https://doi.org/10.1007/s00466-010-0522-0.

Shimizu, Y, Khayyer, A, and Gotoh, H (2022). "An Implicit SPH-based Structure Model for Accurate Fluid–Structure Interaction Simulations with Hourglass Control Scheme," *Eur J Mech B/Fluids*, 96, 122–145. https://doi.org/10.1016/j.euromechflu.2022.07.007.

Uekermann, B, Bungartz, H-J, Yau, LC, Chourdakis, G, and Rusch, A (2017). "Official preCICE Adapters for Standard Open-Source Solvers," *Proc 7th GACM Colloquium Comput Mech Young Scientists Acad*, Stuttgart, Germany. https://www.researchgate.net/publication/321289778.

Walhorn, E, Kölke, A, Hübner, B, and Dinkler, D (2005). "Fluid–Structure Coupling Within a Monolithic Model Involving Free Surface Flows," *Comput Struct*, 83(25–26), 2100–2111. https://doi.org/10.1016/j.compstruc.2005.03.010.

Wu, J, Zhang, G, Jiang, Y, and Yang, X (2022). "Numerical Simulations on the Flooding into a Damaged Cabin with a Flexible Bulkhead Based on the Mixed-Mode Function-Modified MPS Method," *J Mar Sci Eng* 10(11), 1582. https://doi.org/10.3390/jmse10111582.

Xiao, J, Liu, J, Han, B, Wan, D, and Wang, J (2024). "A Two-Way Coupled Fluid–Structure Interaction Method for Predicting the Slamming Loads and Structural Responses on a Stiffened Wedge," *Phys Fluids,* 36, 077123. https://doi.org/10.1063/5.0212806.

Xin, J, et al. (2023). "An Efficient Large-Deformation Fluid-Structure Interaction Model for Flow Induced Oscillation of an Elastic Thin Structure," *Ocean Eng*, 278, 114348. https://doi.org/10.1016/j.oceaneng.2023.114348.

Yang F, Gu, X, Xia, X, and Zhang, Q (2022). "A Peridynamics-immersed Boundary-Lattice Boltzmann Method for Fluid-Structure Interaction Analysis," *Ocean Eng*, 264, 112528. https://doi.org/10.1016/j.oceaneng.2022.112528.

Yang, X, Liu, M, Peng, S, and Huang, C (2016). "Numerical Modeling of Dam-Break Flow Impacting on Flexible Structures Using an Improved SPH–EBG Method," *Coastal Eng*, 108, 56–64. https://doi.org/10.1016/j.coastaleng.2015.11.007.

Yilmaz, A, Kocaman, S, and Demirci, M (2021). "Numerical Modeling of the Dam-Break Wave Impact on Elastic Sluice Gate: A New Benchmark Case for Hydroelasticity Problems," *Ocean Eng*, 231, 108870. https://doi.org/10.1016/j.oceaneng.2021.108870.

Zhang, G, Zha, R, and Wan, DC (2022). "MPS-FEM Coupled Method for 3D Dam-Break Flows with Elastic Gate Structures," *Eur J Mech B/Fluids*, 94, 171–189. https://doi.org/10.1016/j.euromechflu.2022.02.014.

Zhang, W, Wang, J, Guo, H, Liu, Y, and Wan, D (2025). "Numerical Investigations of Ship Hydroelasticity of a 20,000 TEU Containership Based on CFD-MBD Method," *Ocean Eng*, 317, 120061. https://doi.org/10.1016/j.oceaneng.2024.120061.

Zhao, L, Di, Y, and Mao, J (2024). "A Coupled FDEM-IBM-Level Set Method for Water Entry of Multiple Flexible Objects," *J Comput Phys*, 516, 113290. https://doi.org/10.1016/j.jcp.2024.113290.

Zheng, Z, Duan, G, Mitsume, N, Chen, S, and Yoshimura, S (2020). "An Explicit MPS/FEM Coupling Algorithm for Three-Dimensional Fluid-Structure Interaction Analysis," *Eng Anal Bound Elem,* 121, 192–206. https://doi.org/10.1016/j.enganabound.2020.10.002.